Mech. Adv. Technol., Vol. 9, No. 3, 2025, pp. 298–308

DOI: 10.20535/2521-1943.2025.9.3(106).333347

UDK 658.5

Comparison and Evaluation of Conventional and Machine Learning-Assisted Reverse Engineering Workflows

Artem Kunytsia[1] • **Yuliia Lashyna**[1]

Received: 23 July 2025 / Revised: 15 August 2025 / Accepted: 8 September 2025

Abstract: *Reverse engineering workflows play a crucial role in converting physical components into digital CAD models, impacting efficiency and accuracy in various industries. Traditional manual approaches, while highly precise, are often slow and resource-intensive, prompting exploration of machine learning (ML) methods promising accelerated results. The aim of this study is to perform a comparative overview and practical evaluation of conventional and ML-assisted reverse engineering workflows, identifying their accuracy, speed, and applicability to support evidence-based recommendations for workflow selection. As part of the study, a steel chuck-jaw was scanned using a high-precision scanner as an example of a part for reverse engineering. Three distinct CAD models were created: the first by manual surfacing in CATIA V5, the second by semi-automatic fitting in Geomagic Design X, and the third using the ML-based Point2CAD pipeline followed by post-processing in Geomagic Design X. The models were then assessed by comparing surface-to-cloud deviations and the total time required for reconstruction. The manual CATIA workflow achieved the best accuracy but demanded significant time and hands-on effort. The semi-automatic Geomagic workflow offered an effective balance between accuracy and efficiency. The Point2CAD approach dramatically reduced reconstruction time but resulted in significant local deviations, even though the overall geometry was acceptably maintained. These results suggest selecting manual workflow for tasks where accuracy is critical, semi-automatic workflow can be recommended for standard precision tasks with balanced effort, and ML-assisted workflow – for rapid prototyping or digital archiving when moderate inaccuracy is permissible and the necessary hardware is available. Additionally, the comparative overview underscores that selecting a suitable reverse engineering workflow depends significantly on project-specific requirements, particularly regarding required accuracy, available hardware, and acceptable processing time.*

Keywords: *reverse engineering; point cloud; CAD reconstruction; machine learning; workflow selection; dimensional accuracy.*

Introduction

Reverse engineering, a critical link between physical objects and their digital representations, holds significant relevance in modern design, manufacturing, and preservation across diverse sectors. Industries from aerospace and automotive to biomedical, consumer electronics, cultural heritage, and marine utilize its processes for creating digital twins, functional prototyping, and streamlining spare part production. Scientific inquiry in this domain is driven by the continuous need for more effective, precise, and robust methods to address difficulties in reconstructing complex, damaged, or legacy components.

✉ *A. Kunytsia*
kunytsiaartem@gmail.com

[1] *Igor Sikorsky Kyiv Polytechnic Institute, Kyiv, Ukraine*

Investigations into these workflows are vital for improving the throughput, fidelity, and automation of converting scanned data into usable digital models, notably Computer-Aided Design (CAD) representations. Current studies highlight a trade-off between reverse engineering pipelines that prioritize manual, CAD-centric modeling for high accuracy and those that leverage greater automation for increased speed. The practical necessity for advancements stems from demands for faster product development, reproduction of parts lacking original documentation, and integration of digital processes into modern manufacturing, including additive manufacturing. Such developments enable industries to adapt to evolving design requirements and maintain legacy systems.

The core scientific challenge involves developing and evaluating reverse engineering methodologies that can balance competing demands for precision, speed, required expertise, and resilience to imperfections in scanned data.

The potential of Artificial Intelligence (AI) and Machine Learning (ML) to automate key stages like point cloud segmentation and feature recognition is currently being explored. While these data-driven techniques show promise in accelerating the scan-to-CAD cycle, issues persist in handling noisy or incomplete data and ensuring the topological consistency and geometric integrity required for critical applications. Therefore, continued investigation is crucial to refine these methods and develop hybrid pipelines that leverage the strengths of both traditional and emerging approaches.

In summary, enhancing reverse engineering workflows is highly significant for modern industry and technology. The outcomes of such studies are essential for devising more efficient and dependable means of creating digital models from physical objects, which in turn supports innovation, accelerates manufacturing, and facilitates the maintenance and preservation of valuable components and objects across numerous sectors.

Literature review

In current practice, reverse-engineering workflows include accuracy-oriented "conventional" methods and speed-oriented "sustainable" approaches. "Conventional" reverse engineering, as detailed in study [1], focuses on creating a highly accurate Analytical Standard (AS) – a digital model of ideal geometry from the physical object using 3D scanning and CAD tools to ensure specified geometric precision. In contrast, "sustainable" reverse engineering, also explored in study [1], prioritizes rapid production by directly using the processed scan data (often an STL file) for manufacturing (e.g., via 3D printing or CNC machining), bypassing the creation of a detailed AS. Study [1] empirically demonstrates that while constructing a watertight AS model through conventional reverse engineering yields the tightest tolerances for complex aerospace castings, direct manufacturing from an STL model accelerates lead time by approximately eight hours but incurs deviations ranging from –0.30 mm to +0.23 mm, particularly on angled features and in areas with complex geometries like corners and small radii. This trade-off underscores that method selection pivots on allowable tolerance bands, resource availability, and schedule pressure, a dilemma that will continue to influence industrial decision-making until hybrid solutions fully mature.

When legacy components are no longer commercially available, hybrid scan-and-analysis procedures remain indispensable. Paper [2] show that laser digitisation of a broken motor impeller, followed by ANSYS-assisted shape optimisation, enables functional prototyping without original drawings. Nevertheless, their workflow depends on high-precision scanning hardware and extensive manual smoothing–steps that inflate cost for parts with intricate curvature. As a result, the economic viability of such projects still hinges on either reduced scanner prices or the introduction of automated noise-suppression algorithms.

The approach utilizing a minimalist five-step abstraction [3] that simplifies objects by describing them with elementary geometric shapes, which are then represented by simulated planar point clouds, can reduce operator workload, particularly when achieving perfect geometric fidelity is not the primary goal. As demonstrated in [3] dense point-cloud handling is replaced with planar slices, thereby lowering computational overhead while maintaining sub-millimetre error for prismatic parts. Yet, the scheme risks oversimplifying fillets and free-form blends, leading to post-hoc CAD edits when functional surfaces demand tighter conformance. Future refinements could include adaptive slice thickness selection guided by curvature metrics, preserving fine detail without re-introducing heavy point cloud processing.

For extensive free-form surfaces, rapid reconstruction is achievable when robust pre-alignment is ensured. Study [4] combines Iterative Closest Point (ICP) registration with chord-deviation filtering to reconstruct propeller blades and complex hull sections, markedly reducing manual modelling effort. The authors caution that the workflow still relies on a good initial pose: if the starting alignment is poor or occlusions are significant, the algorithm may converge to sub-optimal solutions, so further enhancement of the coarse-alignment stage remains an open task.

Integrating non-contact scanning with additive manufacturing can shorten the spare parts pipeline by bypassing conventional machining; however, this integration demands operator judgement during feature recovery. Work reported in [5] reproduces an automotive distributor cover using a 3D scanner and 3D printing, achieving dimensionally "near-net-shape" results. However, dimensional errors were significant for certain features; hole diameters showed errors over 16 % because the scanner could not detect the deep holes, requiring manual reconstruction in CAD software. Nonetheless, reflective surfaces forced multiple rescans, highlighting the need for systematic scan path planning or the application of anti-glare coatings, both of which lengthen the preprocessing phase.

Extensive mesh healing can jeopardise functional tolerances when symmetry or sealing planes are integral to component performance. In a case study on a ship-shaft housing, the digital reconstruction process resulted in a final CAD model that, when compared to the original scan data, had an average deviation of 0.59 mm and a maximum deviation of 7.66 mm to ensure the component meets its constructional requirements. The authors attributed this large maximum deviation to the lack of symmetry in the initial handmade prototype, which was created with an imprecise manufacturing technology. These findings led the authors to conclude that an alternative production process was advisable to ensure the final component could meet its constructional requirements.

Across diverse fields including aerospace, automotive manufacturing, consumer product design, reverse engineering functions as a bridge to create digital models from physical objects. Review [7] catalogues these imple-

mentations and notes that while overseas researchers have focused on optimizing software, domestic research has focused on high-precision scanning equipment. The paper concludes that the technology's future promises wider industrial application, reduced development costs, and stronger intellectual property protection.

Collectively, studies [1]–[6] reveal that manual, CAD-centric pipelines remain reliable but are inherently labour intensive and error-prone. Fig. 1 outlines the eight-step reverse-engineering workflow, structured into four main phases: (*A*) scanning & preparation, (*B*) iterative surface reconstruction, (*C*) validation, and (*D*) export. The process includes two critical decision gates – evaluating watertightness of the B-Rep and dimensional-error thresholds (deviation (Δdev) between the CAD model and the point cloud is at or below the tolerance threshold τ) – triggering iterative feedback loops when tolerances are exceeded. These iterative rework cycles represent the primary bottleneck in the workflow, highlighting them as ideal candidates for ML-driven automation.

Whereas studies [1]–[6] highlight manual, CAD–centric workflows, recent advances in AI and ML are reshaping the field. Data-driven point cloud segmentation has become a pivotal first step toward automating reverse engineering pipelines.

Point cloud segmentation with deep networks has begun to remove much of the manual effort traditionally required in reverse-engineering workflows. Study [8] presents PointNet, a network that learns permutation-invariant features directly from unordered point sets, while PointNet++ in [9] extends this idea with a hierarchical, multi-scale architecture that captures local geometric context. Although PointNet++ introduces mechanisms to cope with highly non-uniform sampling densities, further robustness is still an active research topic.

Machine learning approaches can now infer parametric patches rather than merely labelling points. Study [10] fits B-spline and analytic primitives via ParSeNet's differentiable pipeline, which is designed to retain local detail and global coherence. However, spline fitting remains sensitive to noise and sparse sampling, especially in high-curvature areas, and producing seamless boundaries remains a challenge. The authors suggest that generating training data that simulates more realistic scan noise is an important direction for future work.

A learning-based approach can recognize engineering features such as holes and slots directly from a CAD mesh model. Study [11] using this method on standard benchmark mechanical parts reported a high testing accuracy of 97.90 %. The method employed discrete Gauss map signatures as a compact representation of shape features and used a random forest classifier for the machine learning model. A key advantage was the significantly reduced training cost; the proposed model took only 3.19 seconds

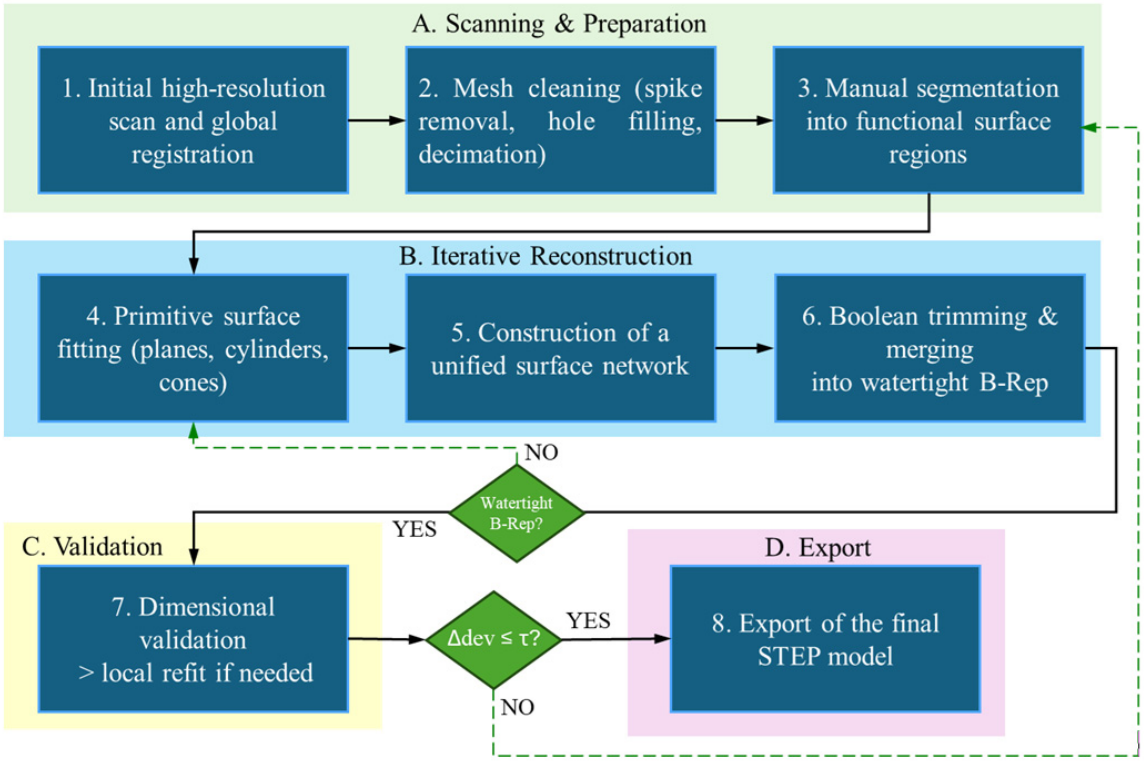

Fig. 1. Manual reverse-engineering workflow: four phases, eight tasks, and two decision loops

to train, a fraction of the time required by more complex 3D Convolutional Neural Networks (CNNs). This approach also requires less memory and has fewer hyperparameters to tune compared to network-based methods.

Topology constrained networks improve structural validity over naively fitted primitives. As presented in [12], the ComplexGen method generates boundary representation (B-rep) chain complexes to simultaneously minimize geometric error and enforce consistency. This holistic modelling approach demonstrates robustness on noisy and partial point clouds when compared to segmentation-based techniques, which are more sensitive to local data quality. However, the framework's reliance on solving a large-scale integer linear program for the final complex extraction introduces a significant computational bottleneck – averaging over nine minutes per model – which may limit its practical application for highly complex parts or in time-sensitive production environments.

For extrusion-dominated parts, learning-guided decomposition into parametric cylinders offers editability in commercial CAD packages. Point2Cyl project, presented in [13], recovers axis, profile, and extent, delivering CAD-native output but relying on a synthetic training corpus that under-represents free-form features. Consequently, the network's generalisability to organically shaped consumer-product casings remain uncertain.

Beyond geometry, some models now emit editable CAD code. CAD Recode project, described in [14] fine-tune a large language model to translate point clouds into CadQuery scripts, bridging reverse engineering and parametric design; success, however, depends on the fidelity of a million-sample synthetic dataset, and cross-domain transfer is still challenging.

Hybrid pipelines blend ML segmentation with analytic and neural surface fitting to capture both primitives and free-form patches. The Point2CAD project, presented in study [15], pairs primitive detection with a novel implicit neural representation for freeform surfaces, intersecting the resulting patches to recover a watertight B-rep that surpasses prior methods on the ABC benchmark. However, the pipeline's performance is highly sensitive to the quality of the initial point cloud segmentation; the authors note that outliers in the predicted point clusters can adversely impact the subsequent surface fitting and topology reconstruction stages.

Collectively, these systems demonstrate that deep learning can shorten the scan-to-CAD cycle from hours to minutes while preserving design intent (see Table 1 for a comparison).

Yet, data-driven routes still come with caveats: they need large, carefully curated datasets and substantial GPU resources. Furthermore, while some models are designed specifically to be robust against noise and partial data, their performance can be impacted by scan quality and unfamiliar material properties like surface reflectivity. Each method also targets a specific CAD representation-extrusion sets, CadQuery scripts, or mixed B-Reps – complicating interoperability across heterogeneous industrial workflows.

Table 1. Comparison of four ML-based projects (ComplexGen, Point2Cyl, CAD Recode, Point2CAD)

Characteristic	ComplexGen	Point2Cyl	CAD Recode	Point2CAD
Input data format	Unstructured point cloud	Unstructured point cloud	Unstructured point cloud	Unstructured point cloud
Primary analytical task	Detects geometric primitives (corners, curves, patches) and their topological relationships	Decomposes a point cloud into a set of "extrusion cylinders," each defined by a 2D sketch and an extrusion path	Translates a point cloud into an executable Python script that reconstructs the CAD model's sketch-extrude sequence	Performs semantic segmentation to partition a point cloud into clusters, then fits primitives to each cluster
Key processing step	Assembles a topologically consistent B-Rep structure via global optimization	Estimates extrusion parameters (axis, extent, sketch profile) for each identified segment	Fine-tunes a Large Language Model (LLM) to autoregressively generate a CadQuery Python script	Intersects fitted surfaces (analytic or freeform) to reconstruct the model's B-Rep topology
Output representation	Parameterized B-Rep CAD model	A set of editable extrusion cylinders loadable into CAD software	An executable Python code script that reconstructs the model	A complete B-Rep CAD model ready for CAM/CAE
Typical use case	Complex mechanical parts with rich topology and tight tolerances	Prismatic parts primarily designed through sketch-and-extrude operations	Automated generation of editable, parametric CAD programs from scanned objects	General-purpose reconstruction of parts with a mix of standard and freeform surfaces

Across research spanning CAD model reconstruction from scan data, direct manufacturing techniques from scans, and learning-based reverse engineering, a clear picture emerges: manual CAD-centric workflows remain viable but scale poorly for damaged, highly intricate, or time-critical parts. Modern ML projects, based on ML algorithms (PointNet variants, ParSeNet, ComplexGen, Point2Cyl, CAD Recode, Point2CAD) show that learned segmentation, parametric fitting, and code generation can drastically reduce re-engineering time while embedding geometric constraints that protect downstream assembly and performance.

In summary, integrating machine learning, especially large language and geometric models into reverse-engineering workflows not only accelerates the creation or repair of editable CAD but also yields models that more faithfully capture functional intent. Future work should explore hybrid pipelines that blend physics-aware priors, self-supervised shape understanding, and prompt-driven LLM reasoning to narrow the gap between scanned reality and production-ready CAD models.

The aim and objectives of the study

The aim of the study is to compare two reverse engineering workflows for scanned parts – a conventional CAD-based process and a hybrid workflow that incorporates ML techniques to quantify differences in dimensional accuracy and total reconstruction time. The practical objective is to outline pathways for further improvement and provide evidence-based recommendations on workflow selection, enabling practitioners to incrementally accelerate and enhance the reliability of part restoration or redesign.

To achieve the aim, the following objectives were set:

1. Build a reference CAD model from the source point cloud using standard reverse engineering tools available in commercial CAD systems.
2. Build an alternative CAD model of the same part by means of a ML-oriented workflow that employs automated segmentation and surface fitting.
3. Compare the resulting models with respect to geometric deviations and overall reconstruction time.
4. Identify the strengths and weaknesses of each workflow in terms of accuracy, speed, required user expertise, and robustness to scan defects.
5. Develop recommendations for selecting the reverse engineering workflow.

The study materials and methods

This study compares two reverse engineering workflows that employ a steel jaw from a three-jaw lathe chuck as the reference component. Every procedure, hardware configuration, software version and data-processing step is documented.

Three-dimensional data acquisition. The part was digitized with a Shining 3D AutoScan Inspec structured-light scanner whose nominal accuracy does not exceed 10 μm.

Conventional CAD workflow. The traditional reconstruction route was executed in CATIA V5 R2021 and Geomagic Design X 2022 on a workstation equipped with an AMD Ryzen 5 3550H (2.10 GHz), 16 GB RAM and an NVIDIA RTX 1660 Ti GPU. Following STL import, global registration was performed, datum planes and cylinders were identified manually, analytic surfaces were fitted, patches were trimmed and merged and, finally, a watertight solid B-Rep model was generated. When using CATIA V5, an engineer relied mainly on interactive surface tools, whereas using Geomagic Design X, an engineer employed Auto-Segment and feature-based wizards that reduced manual input. Reconstruction time was measured with a stopwatch from STL import to STEP export.

ML-assisted workflow. All experiments were performed using Google Colaboratory. The environment utilized Python 3.11.12 and PyTorch version 2.6.0 (built with CUDA 12.4 support). The assigned hardware included an NVIDIA A100-SXM4-40GB GPU, running with NVIDIA driver version 550.54.15 and CUDA version 12.4.

Dimensional verification. Surface-to-cloud deviations were evaluated in Geomagic Design X 2022 with the built-in Accuracy Analyzer, using a sampling density of 0.2 mm and a 3σ statistical filter.

Statistical treatment. For the manual CAD route, two independent timings: one reconstruction in CATIA and one in Geomagic Design X, were recorded without repetition. For the ML route, reconstruction time was averaged over three runs to mitigate GPU runtime variability.

Results of Comparative Workflow Analysis

Manual CAD reconstructions. The reference part is the chuck jaw that combines planar datum faces, cylindrical gripping features and small relief details, offering moderate geometric complexity without excessive intricacy (Fig. 2).

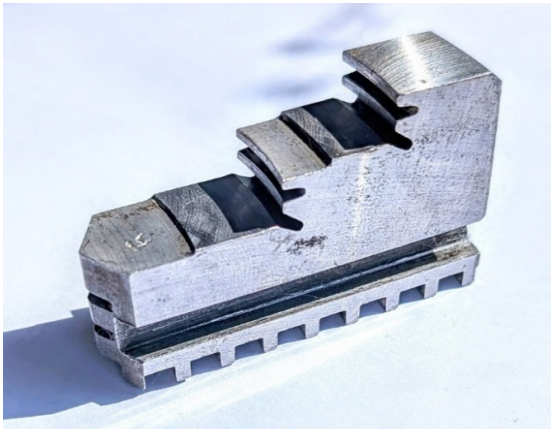

Fig. 2. Steel insert for lathe chuck jaw

The geometry of the part was captured with a structured-light scanner. An antireflective spray was applied beforehand to suppress glare (Fig. 3). The resulting STL mesh contained approximately 5,9 million vertices and 3 million triangular facets.

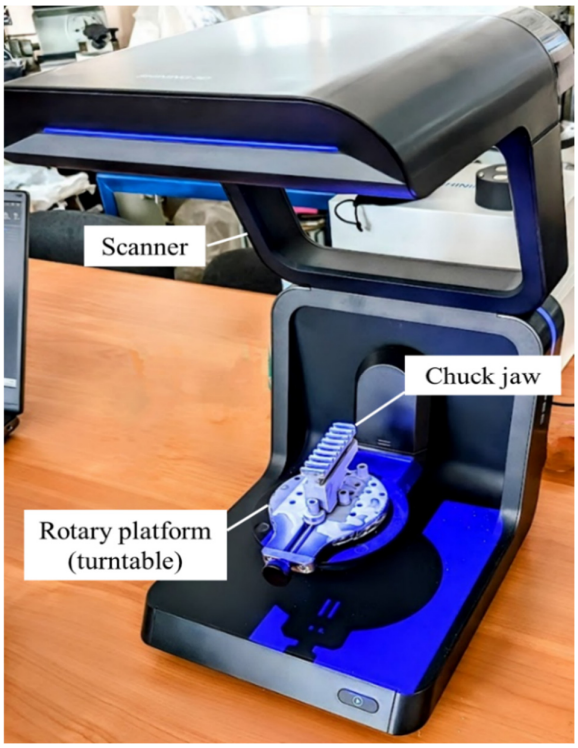

Fig. 3. Scanning procedure with the Shining 3D AutoScan Inspec

Table 2. Accuracy comparison between manually reconstructed CAD models and the reference scan

Metric	CATIA CAD vs. Mesh	Geomagic CAD vs. Mesh
Low tolerance band	−0.10 mm	−0.10 mm
High tolerance band	+0.10 mm	+0.10 mm
Minimum deviation	−0.9663 mm	−0.9145 mm
Maximum deviation	+0.9547 mm	+0.7493 mm
Mean deviation	−0.0311 mm	+0.0044 mm
RMS deviation	0.1922 mm	0.2159 mm
Standard deviation	0.1897 mm	0.2159 mm
Approx. modelling time	≈ 4 h	≈ 3 h

Notes. Statistics were generated with the Accuracy Analyzer tool in Geomagic Design X 2022 using the same ±0.1 mm tolerance window for both reconstructions. Negative values indicate material excess on the CAD model relative to the scan; positive values represent material deficit.

Point-cloud pre-processing. Noise spikes and isolated outliers were removed with statistical filters, after which the mesh was decimated to a uniform point spacing of 0.15 mm to facilitate further operations.

Table 2 summarizes the numerical deviations obtained for the CATIA V5 and Geomagic Design X models. The low- and high-tolerance limits were set to ±0.10 mm for both datasets. Fig. 4 illustrates the spatial distribution of the signed errors: panel (*a*) corresponds to the CATIA model, panel (*b*) to the Geomagic model.

Key values to note in Table 2 include the minimum and maximum deviations (extreme local misfits), the mean and RMS deviations (global geometric fidelity), and the modelling time (workflow effort).

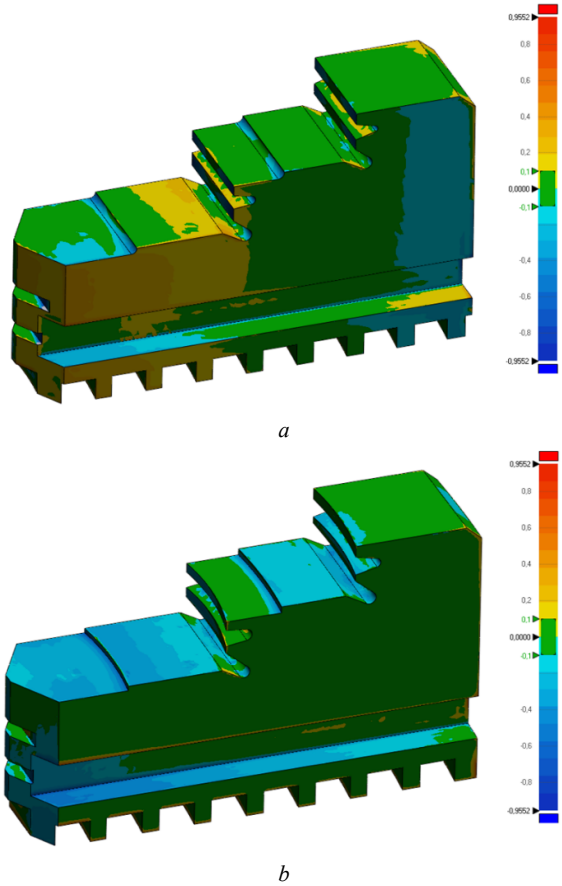

a

b

Fig. 4. Accuracy analyzer visualization: *a* – CATIA CAD vs. Mesh; *b* – Geomagic CAD vs. Mesh

After inspection of the colour plots, attention should be directed to the fillet and slot regions, where the largest local departures are concentrated. A brief numerical commentary is provided beneath the table to reinforce the link between the statistics and the visual error maps.

ML-based reconstruction. Point2CAD cannot ingest a simple XYZ point list; instead, every sample must carry an additional segmentation label s that identifies the

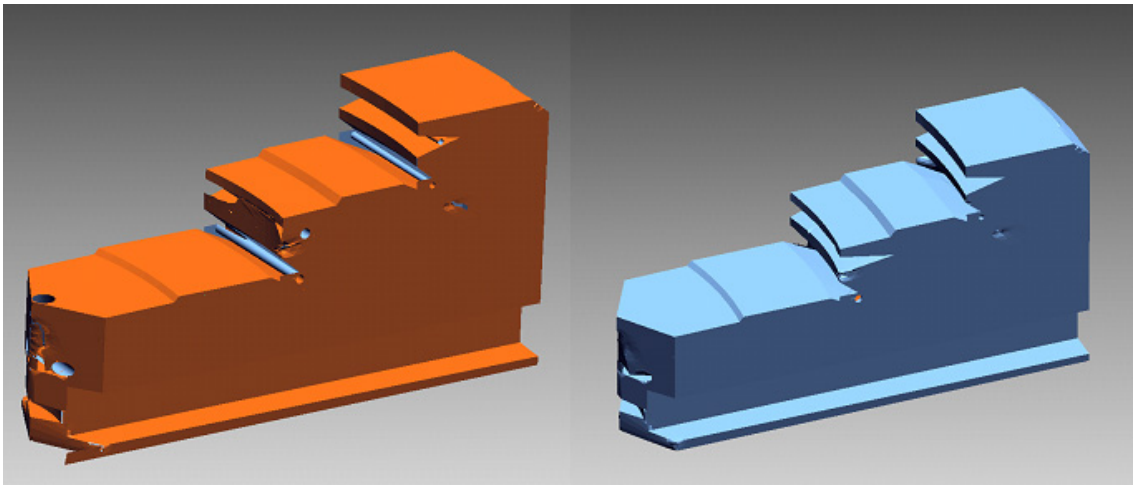

a *b*

Fig. 5. Output from Point2CAD: *a* – before processing; *b* – after processing

Table 3. Accuracy analyzer output for the Point2CAD reconstruction (mesh) compared with the reference scan

Metric	Value (mm)
Low tolerance	−0.10
High tolerance	+0.10
Minimum deviation	−4.318
Maximum deviation	+4.329
Average deviation	−0.035
Root mean square (RMS)	0.355
Standard deviation	0.353
Approx. modelling time	≈ 0.8 h (20 min inference + 30 min repair + 10 min alignment)

surface to which the point belongs (format *x*, *y*, *z*, *s*). As publicly available scans seldom include such labels, a dedicated preprocessing stage was required. Rather than installing and training one of the recommended segmentation frameworks (HPNet or ParseNet), the segmentation was generated in FreeCAD by projecting the manually rebuilt CAD model onto the raw point-cloud and assigning each point to the nearest CAD face through a custom macro.

Because Point2CAD still struggled to converge on the full, highly detailed jaw, the STL was first trimmed to remove the lower serrated rail that mates with the chuck scroll. This simplification reduced geometric complexity and brought the point-count to ≈ 65 000, keeping GPU memory usage within limits. With the down-sampled, pre-segmented cloud, Point2CAD produced an initial mesh in ≈ 20 min; a further ≈ 30 min of post-processing in Geomagic Design X (Healing Wizard, defect removal, re-meshing) were required to repair open edges, fill holes, and replace spurious cylindrical plugs that had been introduced where filleted transitions should appear (Fig. 5).

The mesh exported by Point2CAD was delivered at an incorrect scale and origin offset relative to the reference scan, so a rigid best-fit alignment ≈ 10 min followed by uniform scaling was applied before accuracy analysis.

Although the global mean bias stayed near zero, isolated outliers up to ±4 mm were observed, predominantly in blend regions (Fig. 6).

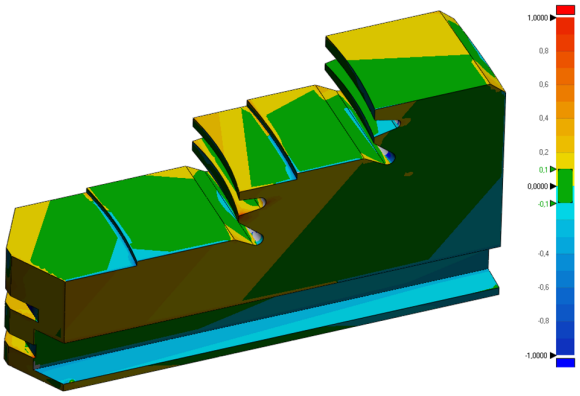

Fig. 6. Accuracy analyzer visualization for the Point2CAD reconstruction (mesh) compared with the reference scan

Head-to-head comparison of workflows. To facilitate an at-a-glance comparison of the three workflows, the key dimensional-accuracy metrics and processing times have been consolidated in Table 4.

A cursory scan of Table 4 therefore indicates a distinct trade-off: the Point2CAD pipeline delivers a usable model almost five times faster than manual surfacing, yet its RMS error is roughly treble that of the CATIA baseline, whereas Geomagic occupies an intermediate position both in terms of cycle time and precision.

Strength and weakness assessment. Table 5 presents the assessment of advantages and disadvantages of the three reverse engineering approaches that utilize aforementioned software tools.

Taken together, the rankings in Table 5 underscore a clear pattern: CATIA excels when maximum fidelity is paramount, Geomagic balances accuracy with moderate effort, while Point2CAD offers unrivalled speed at the cost of local precision-making the choice of workflow heavily case-dependent.

Recommendations for Selecting a Reverse-Engineering Workflow. The most suitable reverse engineering route depends squarely on project priorities. When maximum dimensional fidelity is non-negotiable, a fully manual CAD workflow in CATIA V5 is preferable: its interactive surfacing tools enable sub-millimetre control of datums and features, but this precision comes at the cost of lengthy modelling sessions and the need for highly skilled users.

Table 4. Dimensional-accuracy summary and required efforts for the three reverse engineering workflows

Workflow type	Software/ key automation	Processing time*	Mean dev. (mm)	RMS (mm)	σ (mm)	Min (mm)	Max (mm)	Qualitative remarks
CATIA V5	CATIA V5 (no dedicated RE tools)	≈ 4 h	–0.031	0.192	0.190	–0.966	+0.955	Long modelling phase; labour-intensive surfacing; good global fit but several local "flat-spot" errors where free-hand trimming was required
Geomagic Design X	Geomagic 2022 (Auto Segment. AFR)	≈ 3 h	+0.004	0.216	0.216	–0.915	+0.749	Automated surfacing accelerates workflow; slightly higher spread than CATIA on fillets and slots but all deviations within ±1 mm band
ML-assisted (Point2CAD)	Point2CAD (on A100 GPU) + mesh healing in Geomagic	≈ 0.8 h (20 min inference + 30 min repair & 10 min align/scale)	–0.036	0.355	0.353	–4.318	+4.329	Fully data-driven generation; strong global alignment but large local defects (mis-recognized blends. missing small radii); non-watertight mesh required post-repair; initial scaling & pose mismatch

Table 5. Qualitative strengths and weaknesses of each reverse engineering workflow

Criterion	CATIA V5	Geomagic DX	Point2CAD
Throughput	Slowest	25 % faster than CATIA	Fastest (≈×5)
Required expertise	Skilled surfacer	Intermediate RE skills	Minimal surfacing; GPU needed
Global RMS	0.192 mm	0.216 mm	0.355 mm
Local fidelity	≤±1 mm	≤±1 mm	Up to ±4 mm
Robustness to scan gaps	High (manual judgement)	Moderate (may over-smooth)	Sensitive to mis-labels; healing required
Best-fit bias	Slightly negative	Near-zero	Near-zero
Ideal use-case	Precision-critical assemblies; tight fits	Routine production RE	Rapid ideation / legacy capture

For everyday production tasks where both accuracy and labor intensity matter, Geomagic Design X offers a practical compromise. Its wizard-driven automation shortens modelling time while typically holding global deviations within ±1 mm, making it well suited to teams with intermediate reverse engineering expertise.

Where speed outweighs local surface perfection–such as rapid concept capture, legacy part digitisation for non-critical use, or proof-of-concept designs–an ML-assisted pipeline like Point2CAD delivers a usable model up to five times faster than manual surfacing. Although this approach demands GPU resources and some pre-/post-processing, it tolerates modest geometric inaccuracy and isolated outliers, which is acceptable when turnaround time is the overriding concern.

Discussion of Workflow Performance and Accuracy

The accuracy ranking in Table 4 can be interpreted in practical terms. Manual surfacing in CATIA yielded the smallest RMS error (0.192 mm) but required an entire working day of expert input. Geomagic's semi-automatic workflow increased RMS error by only 0.024 mm while cutting modelling time by roughly 25 %. The Point2CAD pipeline reduced total processing to under one hour, a major improvement in speed, but overall accuracy dropped by a factor of three and isolated errors of several millimetres emerged (Fig. 5b). For tooling parts with a tolerance band of ±0.10 mm, either manual route would pass first-article inspection, whereas the ML result would need local refinement.

Although CATIA delivered the tightest tolerances straight from the default workflow, Geomagic Design X can be tuned to the same accuracy once an expert applies targeted refinement and precision surface-healing operations. Importantly, its semi-automated toolset still keeps total modelling time below that of CATIA.

The effort summary in Table 5 shows that greater speed does not always translate to higher productivity. Point2CAD assumes a workstation equipped with a modern GPU and relies on a non-trivial pre-segmentation step. CATIA, by contrast, runs on standard engineering hardware but occupies a skilled designer for several hours. Geomagic Design X offers a middle ground: it runs on an ordinary CPU and demands less expertise than freehand surfacing.

Spatial error maps (Fig. 4, *a* and *b*) confirm that all reconstructions inherited the wear marks on the clamping face. CATIA's freeform patches tend to smooth over low spots, while Geomagic's AFR under-fits in tight fillets. The ML model, trained on nominal parts, produces small negative spikes in blend areas. These results suggest that automated workflows remain sensitive to scan defects unless training data are augmented with similar artefacts.

The three workflows serve different objectives.

Tasks that demand full dimensional traceability still require manual reconstruction. Maintenance or aftermarket tooling aligns well with the semi-automatic Geomagic path. For rapid concept work or the archiving of legacy parts, the ML workflow delivers a usable starting geometry that can be improved as needed.

Several limitations remain. Only one prismatic sample has been tested; further studies should include freeform and lattice structures. The machine learning pipeline was evaluated offline; end-to-end segmentation and fitting networks such as HPNet or ParSeNet could further reduce user input and should be benchmarked. Finally, functional validation–such as finite-element analysis of clamping loads–has not yet been performed, leaving open the question of whether the observed geometric deviations affect performance.

The adoption of large vision and language models in engineering enables faster geometric reconstruction, which positively impacts both design and manufacturing. In design re-engineering, AI tools reduce manual effort and speed up the development of editable CAD models, freeing engineers to focus on critical features and functional requirements. For manufacturing, AI can help identify feasible production methods by analysing geometric features and suggesting suitable fabrication processes. However, high-precision and complex cases still require expert intervention to ensure technical correctness and manufacturability.

Conclusions

1. Reference models built with standard software – CATIA V5 for fully manual surfacing and Geomagic Design X for semi-automatic fitting – delivered the highest global fidelity. CATIA, in particular, achieved the smallest RMS error and therefore remains the method of choice when precision is mandatory; this level of accuracy, however, comes at the expense of a lengthy reconstruction cycle dominated by meticulous human interaction. With focused refinement passes and high accuracy surface-fitting routines, Geomagic Design X can be tuned to the same tolerance band while still preserving its shorter turnaround time.

2. Introducing a data-driven alternative, the Point2CAD pipeline combined with clean-up operations in Geomagic Design X reduced the overall scan-to-CAD time by roughly a factor of five. The gain stems from the model's automated inference stage, which pushes most geometry identification and primitive placement to the GPU rather than to the designer. Yet this speed comes with a measurable penalty: RMS error rises, and isolated deviations emerge in blend and transition zones, reflecting the network's difficulty in reproducing scan defects and fine local curvature.

3. Placed side by side, the three workflows reveal a clear trade-off between dimensional accuracy and reconstruction time. Manual CAD reconstruction maximises ac-

curacy but demands expert labour; semi-automatic workflow strikes a middle ground suitable for day-to-day production needs; the ML-assisted route enables rapid ideation or quick capture of legacy parts when tight tolerances are not critical.

4. These differences expose the respective strengths and weaknesses of each approach: CATIA excels where the highest dimensional fidelity is required; Geomagic Design X balances precision and processing time; Point2CAD offers unrivalled speed but depends on robust scans, high-end hardware, and post-healing to yield a watertight model.

5. Based on the quantified trade-offs and the distinct strengths and weaknesses identified for each workflow, this study successfully developed and presented evidence-based recommendations. These recommendations provide practitioners with a clear framework for selecting the most appropriate reverse engineering strategy tailored to specific project priorities, such as required precision, acceptable turnaround time, and available user expertise.

Conflict of interest

The authors declare that they have no conflict of interest in relation to this research, including financial, personal, authorship, or any other nature that could affect the research and its results presented in this article.

Use of artificial intelligence

The authors confirm that they did not use artificial intelligence technologies when creating the current work.

References

[1] K. Maiorova, O. Kapinus, and O. Skyba, "Study of the features of permanent and usual reverse-engineering methods of details of complex shapes," *Technology Audit and Production Reserves*, vol. 1, no. 1(75), pp. 19–25, Feb. 2024, doi: https://doi.org/10.15587/2706-5448.2024.297768.

[2] Satish, K.Rambabu, and M. Ramji, "Part Modeling with Reverse Engineering*," International Journal of Engineering Research And*, vol. 2, no. 12, Sep. 2013, [Online]. Available: https://www.ijert.org/research/part-modeling-with-reverse-engineering-IJERTV2IS120297.pdf.

[3] K. Saiga, A. S. Ullah, A. Kubo, and N. Tashi, "A sustainable reverse engineering process," *Procedia CIRP*, vol. 98, pp. 517–522, Jan. 2021, doi: https://doi.org/10.1016/j.procir.2021.01.144.

[4] G. Guan and W.-W. Gu, "reconstruction of propeller and complex ship hull surface based on reverse engineering," *Journal of Marine Science and Technology*, vol. 27, no. 6, p. 2, Jan. 2019, doi: https://doi.org/10.6119/jmst.201912_27(6).0002.

[5] M. I. Yahaya, Z. Samsuddin, A. S. M. Rodzi, Abd. R. Hemdi, M. Othman, and R. M. Noor, "Manufacture of automotive component using reverse engineering and manufacturing additive techniques," *ESTEEM Academic Journal*, vol. 19, no. September, pp. 63–74, Sep. 2023, doi: https://doi.org/10.24191/esteem.v19iseptember.23005.

[6] M. Deja, M. Dobrzyński, and M. Rymkiewicz, "Application of reverse engineering technology in part design for shipbuilding industry," *Polish Maritime Research*, vol. 26, no. 2, pp. 126–133, Jun. 2019, doi: https://doi.org/10.2478/pomr-2019-0032.

[7] T. Wang, "An Overview of the Application of Reverse Engineering in Selected Fields," *Science and Technology of Engineering Chemistry and Environmental Protection*, vol. 1, no. 7, Jun. 2024, doi: https://doi.org/10.61173/g7vycc37.

[8] R. Q. Charles, H. Su, M. Kaichun, and L. J. Guibas, "PointNet: Deep Learning on Point Sets for 3D Classification and Segmentation," Proc. IEEE Conf. Computer Vision and Pattern Recognition (CVPR), pp. 77–85, Jul. 2017, doi: https://doi.org/10.1109/cvpr.2017.16.

[9] C. R. Qi, L. Yi, H. Su, and L. J. Guibas, "PointNet++: deep hierarchical feature learning on point sets in a metric space," arXiv (Cornell University), Jan. 2017, doi: https://doi.org/10.48550/arxiv.1706.02413.

[10] G. Sharma, D. Liu, S. Maji, E. Kalogerakis, S. Chaudhuri, and R. Měch, "PARSENET: a parametric surface fitting network for 3D point clouds," in Lecture notes in computer science, 2020, pp. 261–276. doi: https://doi.org/10.1007/978-3-030-58571-6_16.

[11] L. P. Muraleedharan and R. Muthuganapathy, "A learning-based approach to feature recognition of Engineering shapes," arXiv (Cornell University), Jan. 2021, doi: https://doi.org/10.48550/arxiv.2112.07962.

[12] H. Guo, S. Liu, H. Pan, Y. Liu, X. Tong, and B. Guo, "ComplexGen," *ACM Transactions on Graphics*, vol. 41, no. 4, pp. 1–18, Jul. 2022, doi: https://doi.org/10.1145/3528223.3530078.

[13] M. A. Uy et al., "Point2Cyl: Reverse Engineering 3D Objects from Point Clouds to Extrusion Cylinders," 2022 IEEE/CVF Conference on Computer Vision and Pattern Recognition (CVPR), pp. 11840–11850, Jun. 2022, doi: https://doi.org/10.1109/cvpr52688.2022.01155.

[14] D. Rukhovich, E. Dupont, D. Mallis, K. Cherenkova, A. Kacem, and D. Aouada, "CAD-Recode: Reverse Engineering CAD Code from Point Clouds," arXiv (Cornell University), Dec. 2024, doi: https://doi.org/10.48550/arxiv.2412.14042.

[15] Y. Liu, A. Obukhov, J. D. Wegner, and K. Schindler, "Point2CAD: Reverse Engineering CAD Models from 3D Point Clouds," arXiv (Cornell University), Jan. 2023, doi: https://doi.org/10.48550/arxiv.2312.04962.

Порівняння та оцінка традиційних і заснованих на машинному навчанні робочих процесів зворотного інжинірингу

А. Куниця[1] • **Ю. Лашина**[1]

[1] *КПІ ім. Ігоря Сікорського, Київ, Україна*

Анотація. *Вибір процесу зворотної розробки має суттєвий вплив на ефективність та точність при перетворенні фізичних об'єктів у цифрові CAD-моделі у різних галузях промисловості. Традиційні ручні підходи, хоч і є дуже точними, але часто виявляються повільними та ресурсомісткими, що спонукає розробників до вивчення можливості застосування методів машинного навчання (МН) з метою прискорення робочого процесу.*

Метою цього дослідження є проведення порівняльного аналізу та практичної оцінки традиційних та автоматизованих за допомогою МН процесів зворотної розробки, визначення їх точності, швидкості та застосовності для надання обґрунтованих рекомендацій щодо вибору робочого процесу.

В межах дослідження за допомогою високоточного сканера було відскановано сталевий кулачок патрона в якості прикладу деталі для зворотного проєктування. Було створено три різні CAD-моделі: перша – шляхом ручного відтворення поверхонь у CATIA V5, друга – за допомогою напівавтоматичного методу в Geomagic Design X, і третя – з використанням Point2CAD на основі МН з подальшою постобробкою в Geomagic Design X. Точність отриманих моделей оцінювалась шляхом порівняння відхилення поверхні від вихідної хмари точок. Ефективність робочих процесів порівнювалась на основі аналізу загального часу, необхідного для реконструкції.

Ручний робочий процес у CATIA дозволив досягти найвищої точності, але виявився найбільш тривалим та трудомістким. Напівавтоматичний процес у Geomagic Design X продемонстрував оптимальний баланс між точністю та ефективністю. Підхід, що базується на використанні Point2CAD, значно скоротив час реконструкції, проте призвів до суттєвих локальних відхилень, хоча загальну геометрію виробу було збережено на прийнятному рівні.

Отримані результати свідчать про те, що ручне відтворення поверхонь слід обирати для завдань, де точність є критично важливою, напівавтоматичний робочий процес зворотного проєктування може бути рекомендований для завдань зі стандартною точністю та збалансованими зусиллями, а підходи, засновані на використанні методів машинного навчання, – для швидкого прототипування або цифрового архівування, коли допустима помірна неточність і є в наявності необхідне обладнання. Таким чином, вибір відповідного процесу зворотної розробки значною мірою залежить від специфічних вимог проєкту, зокрема щодо необхідної точності, доступного обладнання та прийнятного часу обробки.

Ключові слова: *зворотна розробка; хмара точок; реконструкція САПР; машинне навчання; вибір робочого процесу; точність розмірів.*